Journal of Magnetism and Magnetic Materials 323 (2011) 3087–3091

Contents lists available at ScienceDirect

Journal of Magnetism and Magnetic Materials

journal homepage: www.elsevier.com/locate/jmmm

Preparation of poly (styrene)-b-poly (acrylic acid)/γ-Fe_2O_3 composites

L.D. Zhang [a], W.L. Liu [a,*], C.L. Xiao [a], J.S. Yao [a], Z.P. Fan [a], X.L. Sun [a], X. Zhang [a], L. Wang [a], X.Q. Wang [b]

[a] School of Materials Science and Engineering, Shandong Polytechnic University, Key Laboratory of Processing and Testing Technology of Glass Functional Ceramics of Shandong Province, Daxue Road, Western University Science Park, Jinan 250353, PR China
[b] State Key Laboratory of Crystal Materials, Shandong University, Jinan 250100, PR China

ARTICLE INFO

Article history:
Received 9 January 2011
Received in revised form
12 March 2011
Available online 30 June 2011

Keywords:
Block copolymer
Nano-iron oxide
Magnetic nanocomposite
Soft magnetism
Atom transfer radical polymerization

ABSTRACT

The use of a block copolymer, poly (styrene)-b-poly (acrylic acid) (PS-b-PAA) to prepare a magnetic nanocomposite was investigated. Poly (styrene)-poly (*t*-butyl acrylate) block copolymer, being synthesized by atom transfer radical polymerization, was hydrolyzed with hydrochloric acid for obtaining PS-b-PAA. The obtained PS-b-PAA was then compounded with the modified γ-Fe_2O_3, and subsequently the magnetic nanocomposite was achieved. The products were characterized by ^{1}H NMR, FTIR, gel permeation chromatography, thermogravimetric analysis, transmission electron microscopy and vibrating sample magnetometer. The results showed that the nanocomposites exhibited soft magnetism, with the mean diameter of 100 nm approximately.

1. Introduction

Magnetic nanoparticles are being extensively studied due to their interesting magnetic properties and technological applications [1]. Meanwhile, polymers have traditionally been considered as excellent host matrices for composite materials. Several advanced polymer nanocomposites have been synthesized with a variety of inclusions such as metals, semiconductors, carbon nanotubes and magnetic nanoparticles [2,3]. The mixing of polymers and nanoparticles provides opportunities to engineer flexible nanocomposites that exhibit magnetic properties [4]. Accordingly, composite materials of polymer and magnetic nanoparticles of iron oxides have attracted considerable attention of the scientific community in recent years because they often encompass the desirable features of both organic and inorganic compounds [5–7], and the very important reason for that seems to be the fact that these materials present high potential of technological applications in several fields, such as enzyme immobilization, magnetic resonance imaging, RNA and DNA purification, cell separation and corrosion protection coatings [8–12].

However, magnetic nanocomposite is difficult to prepare by simple blending or mixing in solution or melt form. Consequently, a great deal of attentions have been placed on block copolymer-nanoparticles nanocomposites since block copolymer can self-assemble into a wide range of ordered nanostructures and nanoparticles can then be sequestered into specified domains to form ordered nanocomposites [13]. Meanwhile, as described in the literature, poly (styrene)-b-poly (acrylic acid) (PS-b-PAA) can form aggregates in aqueous solution, tetrahydrofuran (THF), N, *N*-dimethylformamide, toluene and their mixtures [14]. As a consequence of these, the micelles or aggregates of PS-b-PAA were expected to form nanocomposites with other compounds in organic solvent.

In this work, we have reported the preparation of magnetic nanocomposites using γ-Fe_2O_3 and PS-b-PAA. PS-b-PAA was synthesized by atom transfer radical polymerization (ATRP). ATRP, a successful controlled radical polymerization method [15], as facilitated the preparation of well controlled PS-b-PAA [16] and become the most convenient method that allows the synthesis of well-defined polymers with low polydispersity, specific functionalities and various architectures [17]. Furthermore, we studied the magnetic property of this magnetic nanocomposite, and the results indicated that this composite exhibited soft magnetism. It makes it possible for this composite to be used in many potential applications, such as enzyme immobilization, cell separation and corrosion protection coatings.

2. Experimental

2.1. Materials

Styrene (St) was washed with 1 M aqueous NaOH solution to remove the inhibitor and then with water, after that dried with anhydrous $MgSO_4$ and distilled with CaH_2 under reduced pressure

* Corresponding author. Tel.: +86 531 89631229; fax: +86 531 89631226.
E-mail addresses: wlliu@sdu.edu.cn, liuwl@spu.edu.cn (W.L. Liu).

0304-8853/$ - see front matter © 2011 Elsevier B.V. All rights reserved.
doi:10.1016/j.jmmm.2011.06.062

before use. Cuprous bromide (CuBr) was purified according to the description in literature [18]. Ethyl α-bromoisobutyrate (EBIB), 1,1,4,7, 7-pentamethyldiethylenetriamine (PMDETA), *tert*-butyl acrylate (tBA), THF and γ-Fe_2O_3 (20 nm, 99.5%) were purchased from Shanghai Aladdin Chemical Co. Ltd., China.

2.2. Preparation of PS-b-PAA

First of all, PS was prepared as the macro-initiator by ATRP. A typical preparation procedure of macro-initiator PS is described as follows: a dry round-bottom flask equipped with a three-way stopcock was stowed with St, EBIB, CuBr, PMDETA and cyclohexanone, according to a certain percentage. The flask was sealed and degassed by means of three freeze–pump–thaw cycles, filled with argon and heated at 110 °C for 24 h. The resultant mixture was filtered through a short column of basic alumina (eluent, THF). After removal of THF in vacuo, the residue was dissolved in a small amount of THF, and poured into methanol with vigorous stirring. This process was conducted three times. The precipitate was collected and dried in vacuo, the macro-initiator PS was obtained; secondly, tBA was used as the second step monomers to obtain poly (styrene)-block-poly (*t*-butyl acrylate) (PS-b-PBA) using the same procedure as what is described in the first step. A certain amount of PS-b-PBA, concentrated hydrochloric acid and THF were added to a round bottom flask (100 mL) and heated at 70 °C for 24 h. The mixture was filtered to eliminate mechanical impurities, and the residual impurities were removed with the rotary evaporation apparatus, after that, the product was precipitated in a solution of petroleum ether. The solid, PS-b-PAA, was recovered by filtration and dried in a vacuum overnight. The detailed synthesis process is shown in Scheme 1.

2.3. Preparation of the composite

2.3.1. Modification of nano-iron oxide

In the first step, 6 g of nano-iron oxide was dispersed into 60 mL of ethanol and water (1:1 in volume) under constant stirring. The sample was separated using a permanent magnet after decanting the supernatant. The precipitate was washed three times with ethanol and dried at 40 °C for 10 h. In the second step, adding 120 mL distilled water and 4 g oleic acid into the above vessel, and stirring for 30 min, the modified magnetic nano-iron oxide powder could be obtained, after the same treatment of the product as the first step.

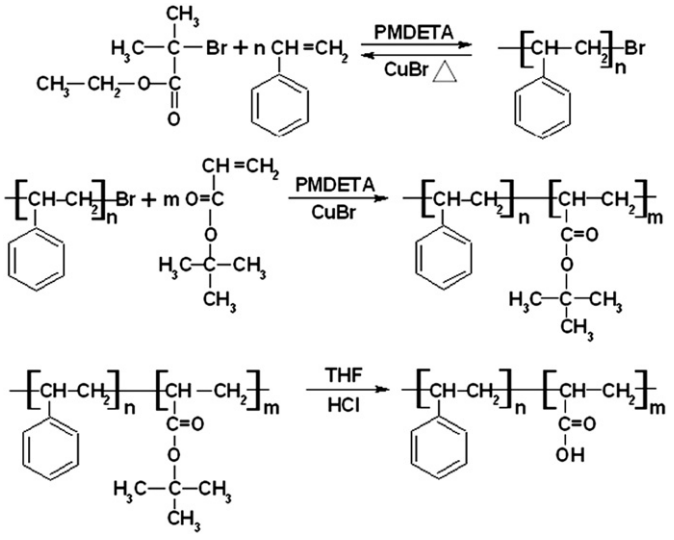

Scheme 1. The synthesis process of PS-b-PAA.

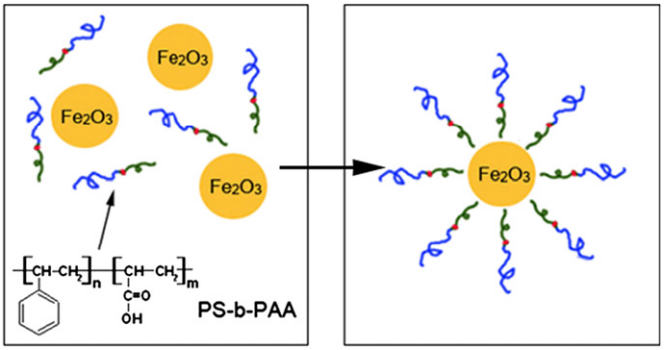

Fig. 1. Schematic illustration for the preparation of magnetic nanocomposites.

2.3.2. Preparation of magnetic nanocomposite

Nano-iron oxide powder (1 g) and PS-b-PAA (2 g) were mixed with 10 mL THF. Then 20 mL distilled water was added to the above reaction medium at the rate of 2 mL/min while stirring. The filtering solids were washed thoroughly with petroleum ether, and then dried in vacuum for 24 h to obtain magnetic nanocomposite. The preparation of magnetic composite is shown in Fig. 1, which shows that the nano-iron oxide particles were coated with PS-b-PAA.

2.4. Characterization

^{1}H NMR (400 MHz) spectra were recorded on a Bruker AVANCE spectrometer with $CDCl_3$ as solvent at room temperature. Fourier transform infrared (FTIR) spectra were obtained using a Nicolet EXUS 470 FTIR spectrophotometer. Gel Permeation Chromatography (GPC) was performed with a Waters 150 C detector. Measurements on GPC were performed in THF solvent at 45 °C with a 1.0 mL/min flow and calibration based on a set of monodisperse polystyrene standards. The morphology and size distribution of the particles were examined by transmission electron microscope (TEM) using a JEM-1011 at an accelerating voltage of 100 kV. Thermogravimetric analysis (TGA) was performed with an STA-449C apparatus under nitrogen gas at a flow rate of 25 cm^3/min, and the heating rate was 10 °C/min. The magnetic properties of the magnetic nanocomposite samples were measured using a Lake shore-7410 vibrating sample magnetometer (VSM).

3. Results and discussion

3.1. Analysis of PS-b-PAA

3.1.1. ^{1}H NMR spectra of PS, PS-b-PBA and PS-b-PAA

A typical ^{1}H NMR spectrum, shown in Fig. 2, confirms the formation of the polymers. As shown in Fig. 2(a), the peaks at 6.3–7.2 ppm originate from the hydrogen atoms on the benzene ring; the peaks at 1.2–2.3 ppm are attributed to the hydrogen atoms on methyl and methylene groups.

Fig. 2(b) shows the ^{1}H NMR spectra of the PS-b-PBA. In addition to the large peaks of the repeated units of tBA at 1.48 ppm and the large peaks of the protons of main chain repeated units from 1.2 to 2.3 ppm, the polymer showed the characteristic signals of the phenyl proton of St repeated units at 6.3–7.2 ppm. But in Fig. 2(c), the signal at 1.48 ppm, attributed to the *tert*-butyl protons of the PBA block, disappeared completely, and the peak appeared at 11.0 ppm, which attributed to carboxyl proton. These indicate that the PS-b-PBA had successfully transformed into PS-b-PAA.

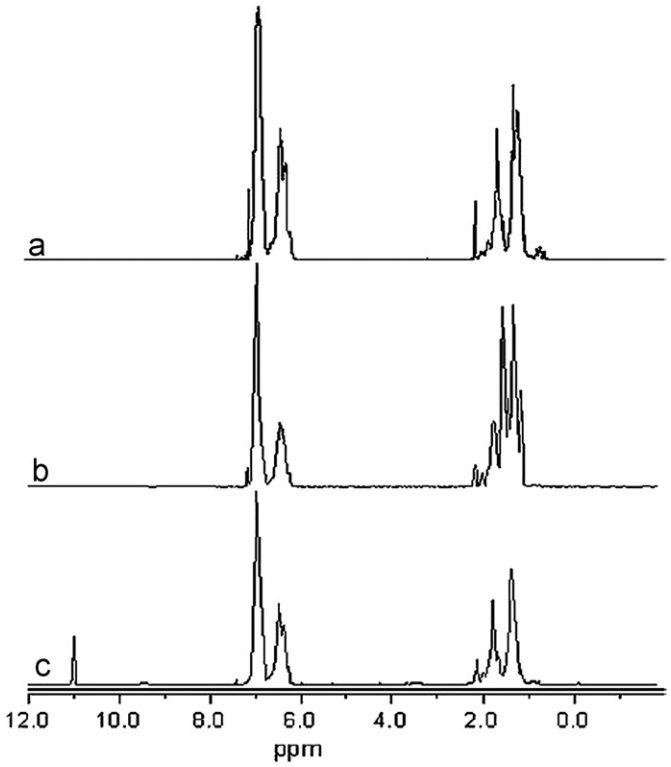

Fig. 2. ^{1}H NMR spectra of (a) PS, (b) PS-b-PBA and (c) PS-b-PAA.

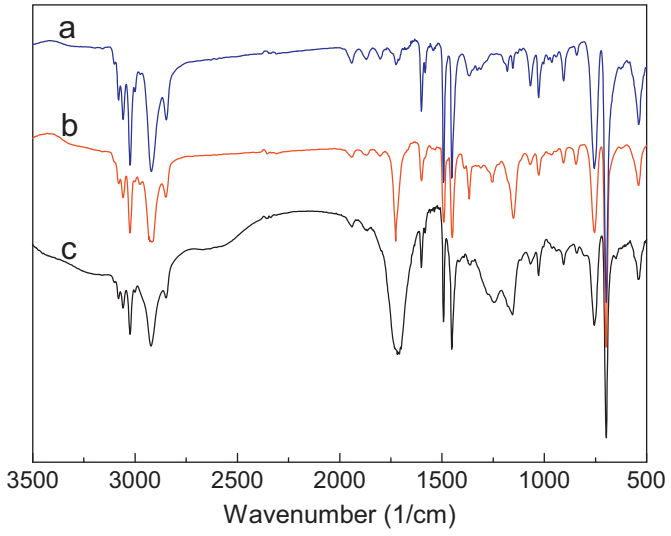

Fig. 3. FTIR spectra of (a) PS, (b) PS-b-PBA and (c) PS-b-PAA.

3.1.2. FTIR spectra of PS, PS-b-PBA and PS-b-PAA

Fig. 3 is the FTIR spectra of PS, PS-b-PBA and PS-b-PAA. From Fig. 3(a), the absorptions at 2920–3080, 1454–1601, 696 and 756 cm^{-1} are characteristic of the benzene ring. By comparing Fig. 3(a) and (b), two additional absorption peaks appeared at 1370 and 1726 cm^{-1}, which belong to *tert*-butyl and the C=O bond of ester group, respectively. Compared to Fig. 3(b), the strong absorptions between 3000 and 3500 cm^{-1} of carboxyl group appeared clearly, and the characteristic absorption of *tert*-butyl at 1370 cm^{-1} disappeared as shown in Fig. 3(c). These indicate that the PS-b-PBA has been hydrolyzed.

Table 1
The GPC results of PS-b-PBA and PS-b-PAA.

Samples	M_n	M_w	PDI=M_w/M_n
PS-b-PBA	29,100	38,500	1.32
PS-b-PAA	24,800	32,500	1.31

3.1.3. GPC spectra of PS-b-PBA and PS-b-PAA

The GPC results of PS-b-PBA and PS-b-PAA are shown in Table 1. It can be seen that the number (M_n) and average molecular weight (M_w) of PS-b-PAA decreased compared with PS-b-PBA, and the PDI (polydispersity index) is small. This result shows that PS-b-PBA has been hydrolyzed. The ^{1}H NMR, FTIR and GPC results indicated that the PS-PAA block copolymer was obtained.

3.2. Analysis of magnetic nanocomposite

3.2.1. TEM study

According to the TEM images in Fig. 4, the raw γ-Fe_2O_3 and magnetic nanocomposites can be approximated as spheres with mean diameters of 20 and 100 nm, respectively. From Fig. 4b and c, the PS-b-PAA coating was observed as a layer surrounding the γ-Fe_2O_3, exhibiting larger solid particles. The phenomena are responsible for the observed morphology in the samples as shown in Fig. 1.

3.2.2. TGA study

TGA curve for the nano-iron oxide is shown in Fig. 5(a). The first thermal decomposition, which starts at 70 °C and ends at 130 °C with weight loss of 2.85% from the sample initial weight, resulted from the release of both free water and structure water. The second stage, continues up to 420 °C with weight loss of 3.01%, which might be due to the loss of the residual impurities.

As for the oleic acid modified nano-iron oxide, which is shown in Fig. 5(b), the first weight loss (8%) that occurred at 179–236 °C can be ascribable to disassembling of linking chains between iron gel and ethanol or oleic acid [19,20]. The second weight loss (8.22%) at 256–313 °C is considered to arise from decomposition of the residual oleic acid. The third weight loss (13.11%) that occurred at 366–471 °C is ascribable to carbonation loss.

Similar changes for magnetic nanocomposite also occurred as shown in curve (c) of Fig. 5. The water and ethanol desorbed at 80–195 °C with weight loss of 4.32%, while the residual oleic acid and organic matter decomposed with weight loss of 10.1% and 22.23% at 216–313 and 400–461 °C, respectively.

Furthermore, it can be figured out that the total weight losses for nano-iron oxide, oleic acid modified nano-iron oxide and magnetic nanocomposite are of 5.86%, 29.33% and 42.59%, respectively. This is mainly attributed to the existence of organic material. Therefore, the quantity of nano-iron oxide can be estimated from the residue at 550 °C [21], that is, it can be concluded that the amount of γ-Fe_2O_3 in the magnetic nanocomposite is about 57%.

3.2.3. Magnetization study

The hysteresis loops reflect intrinsic features of ferromagnets. Its ready appearance under simple conditions makes it not only technologically important, but also a theoretical challenge [22]. Remanent magnetization is the visible proof of magnetic hysteresis, because the magnetization, lagging behind the applied field, cannot decrease to zero when this is released, even when the external field is removed, the magnet will retain some field.

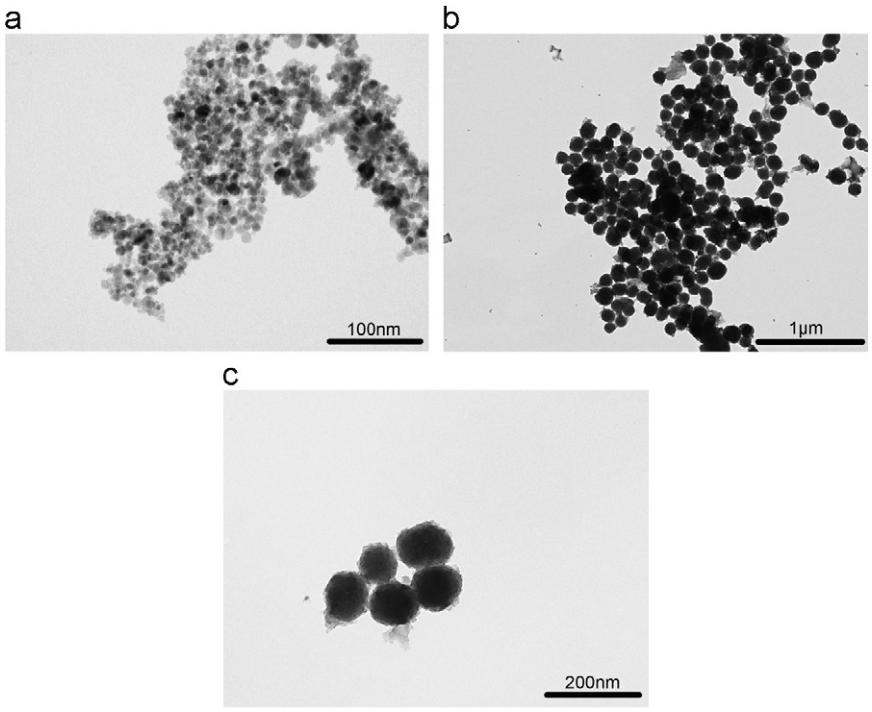

Fig. 4. TEM images of (a) the raw γ-Fe_2O_3 and (b, c) magnetic nanocomposites.

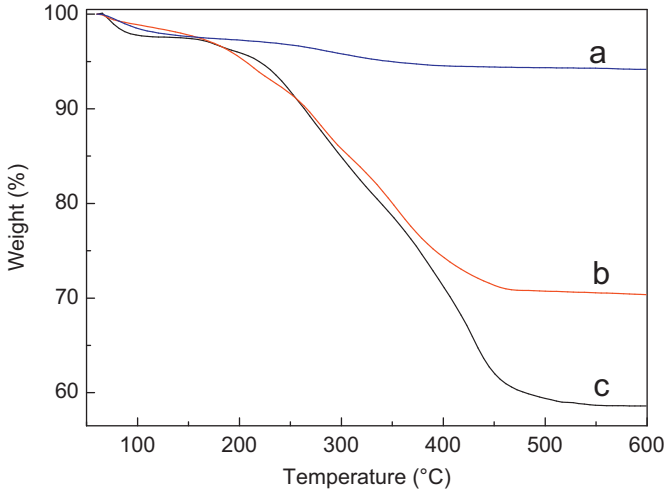

Fig. 5. The TGA curves of samples: (a) nano-iron oxide, (b) oleic acid modified iron oxide and (c) magnetic nanocomposites.

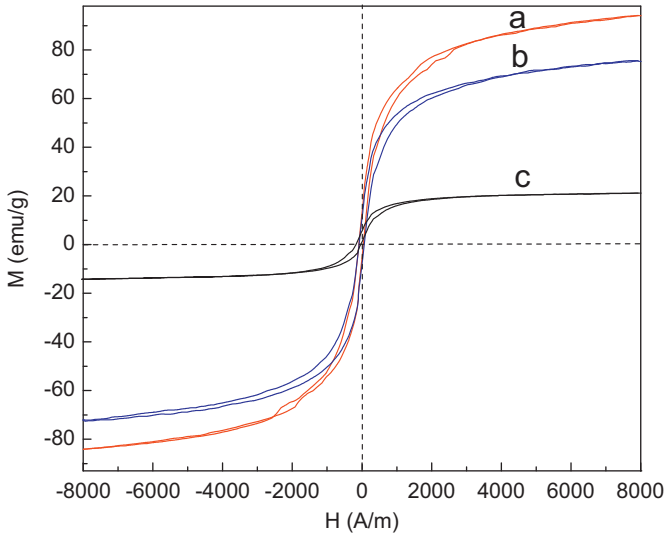

Fig. 6. The hysteresis loop spectra: (a) nano-iron oxide, (b) oleic acid modified iron oxide and (c) magnetic nanocomposite.

Fig. 6 shows the room temperature magnetic hysteresis of nano-iron oxide oleic acid modified iron oxide, and magnetic nanocomposite over the field range −8000–8000 A/m. The value of magnetization sharply increases with the external magnetic field strength at low field region. For all samples, a typical soft magnetic "S"-like shape of hysteresis loops was observed at room temperature. Those "S"-like shape loops can be divided into two parts: linear parts and curvature parts. All of the samples show small hysteretic behavior with a low coercivity (H_c) of 7, 8 and 12 A/m (Table 2), respectively. Table 2 summarizes the reduction of saturation magnetization (M_s) and remanent magnetization (M_r) after nano-iron oxide was modified, which was mainly attributed to the existing and the high content of organic materials.

Because of the existing organic materials, the particles are dispersed, and interaction fields decrease, which enhance the coercivity [23]. A number of theoretical expressions have been derived, which claim to represent the relationship [24]. The most common formula is

$$H_c(p) = H_c(0)(1-p) \quad (1)$$

Table 2
The VSM results of samples.

Samples	M_s (emu/g)	M_r (emu/g)	H_c (A/m)
Nano-iron oxide	94	13	7
Oleic acid modified iron oxide	75	10	8
Magnetic nanocomposites	21	5.52	12

where $H_c(p)$ is the coercivity of the sample, $H_c(0)$ is the coercivity of the isolated particles and p is the packing fraction. Obviously, as p decreases, then $H_c(p)$ increases (Table 2), because of the existence of organic material.

4. Conclusions

The PS-b-PAA/γ-Fe_2O_3 nanocomposites were prepared successfully, which exhibited ferromagnetism at room temperature. The structure and properties of this nanocomposite were characterized by ^{1}H NMR, FTIR, GPC, TEM, TGA and VSM. The results showed that the nanocomposites exhibit soft magnetism (M_s=21 emu/g, H_c=12 A/m), which could be easily magnetized and demagnetized. Moreover, owing to the existing high content of organic matters, the organic matters can provide mechanical and chemical stability to the magnetic nanocomposites. It indicates that the obtained magnetic nanocomposites were promising materials for numerous potential applications fields, including aerospace, electronic information, biomedicine and bioengineering.

Acknowledgments

This work is supported by the Scientific Research Foundation for the Returned Overseas Scholars in Jinan (20100406), the Youth Scientist Fund of Shandong Province (2007BS04007), the Doctoral Startup Foundation of Shandong Institute of Light Industry, National Natural Science Foundation of China (50772059) and the foundation for the author of National Excellent Doctoral Dissertation (no. 200539) for PR China.

References

[1] L.L. Zhou, J.Y. Yuan, W.Z. Yuan, X.F. Sui, S.Z. Wu, Z.L. Li, D.Z. Shen, Synthesis, characterization, and controllable drug release of pH-sensitive hybrid magnetic nanoparticles, J. Magn. Magn. Mater. 321 (2009) 2799–2804.
[2] K.K. Oh, H. Lee, W.S. Lee, M.J. Yoo, W.N. Kim, H.G. Yoon, Effect of viscosity on the magnetic permeability of Sendust-filled polymer composites, J. Magn. Magn. Mater. 321 (2009) 1295–1299.
[3] J.L. Wilson, P. Poddar, N.A. Frey, H. Srikanth, K. Mohomed, J.P. Harmon, S. Kotha, J. Wachsmuth, Synthesis and magnetic properties of polymer nanocomposites with embedded iron nanoparticles, J. Appl. Phys. 95 (2004) 1439–1443.
[4] G.Z. Wu, X.X. Cai, X.J. Lin, H. Yui, Heterogeneous distribution of magnetic nanoparticles in reactive polymer blends, React. Funct. Polym. 70 (2010) 732–737.
[5] Z.L. Lei, Y.L. Li, X.Y. Wei, A facile two-step modifying process for preparation of poly(SStNa)-grafted Fe_3O_4/SiO_2 particles, J. Solid State Chem. 181 (2008) 480–486.
[6] X. Liu, Y. Guan, H. Liu, Z. Ma, Y. Yang, X. Wu, Preparation and characterization of magnetic polymer nanospheres with high protein binding capacity, J. Magn. Magn. Mater. 293 (2005) 111–118.
[7] R. Sondjaja, T.A. Hatton, M.K.C. Tam, Clustering of magnetic nanoparticles using a double hydrophilic block copolymer, poly(ethylene oxide)-b-poly(-acrylic acid), J. Magn. Magn. Mater. 321 (2009) 2393.
[8] X.B. Ding, Z.H. Sun, G.X. Wan, Y.Y. Jiang, Preparation of thermosensitive magnetic particles by dispersion polymerization, React. Funct. Polym. 38 (1998) 11–15.
[9] E.B. Denkbas, E. Kilicay, C. Birlikseven, E. Öztürk, Magnetic chitosan microspheres: preparation and characterization, React. Funct. Polym. 50 (2002) 225–232.
[10] E. Veličkova, E. Winkelhausen, S. Kuzmanova, M. Cvetkovska, Ch. Tsvetanov, Hydroxyethylcellulose cryogels used for entrapment of Saccharomyces cerevisiae cells, React. Funct. Polym. 69 (2009) 688–693.
[11] C.M. Yang, H.Y. Li, D.B. Xiong, Z.Y. Cao, Hollow polyaniline/Fe_3O_4 microsphere composites: Preparation, characterization, and applications in microwave absorption, React. Funct. Polym. 69 (2009) 137–144.
[12] N. Ahmad, A.G. MacDiarmid, Inhibition of corrosion of steels with the exploitation of conducting polymers, Synth. Met. 78 (1996) 103–110.
[13] K. Char, M.J. Park, Selective distribution of interacting magnetic nanoparticles into block copolymer domains based on the facile inversion of micelles, React. Funct. Polym. 69 (2009) 546–551.
[14] J. Li, Q.L. Zhao, G.Y. Zhang, J.Z. Chen, L. Zhong, L. Li, J. Huang, Z. Mab, Synthesis of monoclinic WO_3 nanosphere hydrogen gasochromic film via a sol-gel approach using PS-b-PAA diblock copolymer as template, Solid State Sci. 12 (2010) 1393–1398.
[15] J.K. Oh, J.M. Park, Iron oxide-based superparamagnetic polymeric nanomaterials: design, preparation, and biomedical application, Prog. Polym. Sci. 36 (2011) 168–189.
[16] Z.L. Lei, S.X. Bi, Preparation and properties of immobilized pectinase onto the amphiphilic PS-b-PAA diblock copolymers, J. Biotechnol. 128 (2007) 112–119.
[17] M. Degirmenci, O. Izgin, A. Acikses, N. Genli, Synthesis and characterization of cyclohexene oxide functional polystyrene macromonomers by ATRP and their use in photoinitiated cationic polymerization, React. Funct. Polym. 70 (2010) 28–34.
[18] Z.J. Wei, W.L. Liu, C.L. Xiao, D. Tian, Z.P. Fan, X.L. Sun, X.Q. Wang, Based on atom transfer radical polymerization method preparation of fluoropolymer superhydrophobic films, Thin Solid Films 518 (2010) 6972–6976.
[19] Q.L. Fan, K.G. Neoh, E.T. Kang, B. Shuter, S.C. Wang, Solvent-free atom transfer radical polymerization for the preparation of poly(poly(ethyleneglycol) monomethacrylate)-grafted Fe_3O_4 nanoparticles: synthesis, characterization and cellular uptake, Biomaterials 28 (2007) 5426–5436.
[20] Z.L. Liu, Z.H. Ding, K.L. Yao, J. Tao, G.H. Du, Q.H. Lu, X. Wang, F.L. Gong, X. Chen, Preparation and characterization of polymer-coated core-shell structured magnetic microbeads, J. Magn. Magn. Mater. 265 (2003) 98–105.
[21] R. Hernández, C. Mijangos, In situ synthesis of magnetic iron oxide nanoparticles in thermally responsive alginate-poly(N-isopropylacrylamide) semi-interpenetrating polymer networks, Macromol. Rapid Commun. 30 (2009) 176–181.
[22] I. Essaoudi, F. Dujardin, A. Ainane, M. Saber, J. Gonzalez, Some nagnetic properties of the amorphous transverse spin-1/2 ising system, Chin. J. Phys. 47 (2009) 729–739.
[23] R. Hernández, G. López, D. López, M. Vázquez, C. Mijangos, Magnetic characterization of polyvinyl alcohol ferrogels and films, J. Mater. Res. 22 (2007) 2211–2216.
[24] J.E. Knowles, Coercivity and packing density in acicular particles, J. Magn. Magn. Mater. 25 (1981) 105–112.